Hindawi Publishing Corporation
Advances in Materials Science and Engineering
Volume 2012, Article ID 730810, 7 pages
doi:10.1155/2012/730810

Research Article

The Influence of Na and Ti on the *In Vitro* Degradation and Bioactivity in 58S Sol-Gel Bioactive Glass

Shirong Ni,[1] Ruilin Du,[2] and Siyu Ni[2,3]

[1] *Department of Pathophysiology, Wenzhou Medical College, Wenzhou 325035, China*
[2] *Biomaterials and Tissue Engineering Research Center, Shanghai Institute of Ceramics, Chinese Academy of Sciences, Shanghai 200050, China*
[3] *College of Chemistry, Chemical Engineering and Biotechnology, Donghua University, Shanghai 201620, China*

Correspondence should be addressed to Shirong Ni, nisiron1022@yahoo.com.cn and Siyu Ni, synicn@yahoo.com.cn

Received 12 February 2012; Revised 8 May 2012; Accepted 25 May 2012

Academic Editor: Delia Brauer

The aim of this study was to investigate the effect of Na and Ti on the *in vitro* degradation and bioactivity in the 58S bioactive glass. The degradation was evaluated through the activation energy of Si ion release from bioactive glasses and the weight loss of bioactive glasses in Tris-HCl buffer solution. The *in vitro* bioactivity of the bioactive glasses was investigated by analysis of apatite-formation ability in the simulated body fluid (SBF). The results showed that Na in the 58S glass accelerated the dissolution rate of the glass, whereas Ti in the 58S glass slowed down the rate of glass solubility. Bioactivity tests showed that Na in glass increased the apatite-forming ability in SBF. In contrast, Ti in glass retards the apatite formation at the initial stage of SBF soaking but does not affect the growth of apatite after long periods of soaking.

1. Introduction

For hard tissue repair, the controlled bioactivity and degradation of materials are required to meet different clinical requirements. However, there are also shortcomings of individual material for its intended medical applications. Then the design of hybrid materials offers an exceptional opportunity to allow good control of material properties.

Bioactive glasses have been studied for more than 30 years since Hench et al. invented melt bioactive glass 45S5 with four components of CaO, SiO_2, Na_2O, and P_2O_5. A new way to obtain bioactive materials is through the low-temperature sol-gel method [1]. The most characteristic sol-gel-derived bioactive glass is the 58S which is a silica-based ternary glass, containing SiO_2, CaO, and P_2O_5 [2]. The rate of surface bone-like hydroxyapatite (HA) formation for the 58S compositions was even more rapid than for melt-derived 45S5 bioglass [3]. This finding offered a potential processing method for molecular and textural tailoring of the biological behavior of a new, third generation of bioactive materials [3]. The study on sol-gel bioactive glasses showed that the *in vitro* bioactivity and degradation was affected by both chemical composition and structure, and various ions such as Na^+ Mg^{2+}, Zn^{2+}, Al^{3+} were introduced into sol-gel glasses to modify the chemical composition and structure [4–7]. Sodium has been reported as network disrupting species in glasses [8]. Titanium is considered to be harmless in contact with human tissue, and it has ever been used as a nucleating agent in glasses [9]. Therefore, a suitable substitution of 58S sol-gel glass with Na or Ti may render it more adjustable in the biological properties. Up to now, few studies have been reported to deal with the influence of Na or Ti substitution on the degradation behavior and bioactivity of the 58S sol-gel glass.

In this study, Na and Ti were introduced into 58S sol-gel glasses, and the influence of Na and Ti on the degradation and deposition of HA in the 58S was evaluated and compared, which may provide more useful information

for better understanding of the properties of these three materials and lead to the design of bone implant biomaterials with improved properties.

2. Materials and Methods

2.1. Preparation and Characterization of Glass Samples. Three sol-gel glasses (58S, 58S6N, and 58S6T) have been synthesized. The chemical compositions are given in Table 1. 58S bioactive glass was prepared using the sol-gel method according to the procedure described by Zhong and Greenspan [10]. The sodium-containing glass (58S6N) was prepared using the sol-gel technique by partial substitution of CaO with Na_2O from a CaO-SiO_2-P_2O_5 bioactive glass (58S). The 58S6N sols were prepared by mixing deionized water, 2N HNO_3, tetraethoxysilane (TEOS, $Si(OC_2H_5)_4$), triethylphosphate (TEP, $OP(OC_2H_5)_3$), calcium nitrate (CN, $Ca(NO_3)_2 \cdot 4H_2O$), and sodium nitrate (NN, $NaNO_3$) in order. The molar ratio of H_2O/TEOS was 10 : 1, and HNO_3 was used as catalyst for the hydrolysis of TEOS and TEP. The titanium-containing glass (58S6T) was also prepared using the sol-gel technique by partial substitution of CaO with TiO_2 from 58S bioactive glass. Briefly, the appreciated amount of tetrabutyl titanate ($Ti(OC_4H_9)_4$) was dissolved in absolute ethanol. To this solution, a mixture of 5N HNO_3 and absolute ethanol was added and stirred at room temperature for several hours. In the mixture, the molar ratio of $Ti(OC_4H_9)_4$ and ethanol was 1 : 15. The TiO_2 sol was then added to the 58S sol to obtain 58S6T sols. The resultant 58S, 58S6N, and 58S6T sols were then aged at 60°C for 72 h and dried at 130°C for 72 h, and the glass powders were obtained after ball milling the dried gels for 24 h and calcination of the gel powders at 700°C for 2 h. After that, the glass powders were uniaxially pressed into disks ($\Phi 6 \times 2$ mm) and isostatically pressed for 30 min with a pressure of 200 MPa. The pressed disks were calcined at 700°C for further experiments. The phase compositions of the sintered samples were characterized by X-ray diffraction (XRD; Geigerflex, Rigaku Co., Japan).

2.2. Dissolution Studies of the Glass Samples. The dissolution behavior of the bioactive glass samples was estimated by soaking them in Ringer's solution (pH = 7.4) at 37°C for 1, 3, 7, and 14 days with a surface area-to-volume ratio of 0.1 cm^2/mL [11]. The solution was renewed every day. At the selected time points, the samples were removed from the solution, gently rinsed with ethanol, and dried at 60°C for 24 h then the final weight of each sample was accurately measured. The weight loss (degradation) was expressed as the percentage of the initial weight. Five samples for each material were tested for each condition. All results were expressed as means ± standard deviation. In order to calculate the activation energy for Si ion release, the ion solubility tests were carried out at 24°C, 37°C, and 55°C by soaking 200 mg of glass in 200 mL of Tris-HCl buffer solution for 6 h. After soaking, the calcium (Ca), silicon (Si), sodium (Na), titanium (Ti), and phosphorus (P) ion concentrations in the fluids were measured by inductively coupled plasma atomic emission spectroscopy (ICP-AES; Varian Co., USA). All results were expressed as mean ± standard deviation from the triplicate samples in each experiment. The activation energy for Si release was calculated according to Arrhenius equation for an ionic diffusion model [12]:

$$\mathrm{Ln}[\mathrm{Si}] = \ln[\mathrm{Si}_0] - \frac{E_a}{RT}. \quad (1)$$

Table 1: Chemical composition of the synthesized bioactive glasses.

Sample	Composition (mol%)				
	SiO_2	CaO	P_2O_5	Na_2O	TiO_2
58S	59	36	5	0	0
58S6N	59	30	5	6	0
58S6T	59	30	5	0	6

2.3. Soaking in Simulated Body Fluid. The apatite formation behavior of the bioactive glass samples was evaluated by soaking them in simulated body fluid (SBF). The SBF compositions were prepared following the technique described by Kokubo et al. [13]. The samples were immersed in SBF (pH = 7.4) with the ratio of surface area (cm^2) to solution volume (mL) of 0.1 cm^2/mL at 36.5°C for 1, 3, and 5 days, respectively [14]. The soaking experiment was carried out in a shaking bath set at 60 rpm. After soaking, the samples were removed from the SBF solution, gently rinsed with acetone, and then dried at room temperature before further characterization. The surface microstructures of the samples after soaking were observed by field emission scanning electron microscopy (FESEM; JSE-6700F, JEOL, Japan). Changes in pH of the solution were measured by a pH testmeter (pHS-3C, Jingke Leici Co., China). Apatiteformation on the materials was characterized with thin-film XRD and Fourier transform infrared reflection spectroscopy (FTIR; Thermo Nicolet Co., USA).

3. Results and Discussion

3.1. Dissolution Studies of the Glass Samples. The XRD patterns of the samples after calcination at 700°C are shown in Figure 1. In order to reduce the interference of the background and noise, XRD patterns have been treated by smoothing. It can be seen that 58S and 58S6T were amorphous, whereas 58S modified by Na (58S6N) showed a higher degree of crystallization compared with 58S. However, it is difficult to assign the crystal phases. Table 2 shows Si ionic concentrations leached from the three glasses after soaking in Tris-HCl buffer solution for 6 hours at 24°C, 37°C, and 55°C, respectively. 58S6N glass released the highest amount of Si at each tested point, whereas 58S6T showed the lowest release of Si ions. 58S glass showed intermediate values between 58S6N and 58S6T. Figure 2 shows the Arrhenius plots for silicon ion release from the glasses, and the activation energy of Si release was obtained from the slope of the curves as shown in Table 3. The 58S6N shows the lowest E_a, 0.18 eV, and the

Table 2: Ionic concentrations of bioactive glasses after soaking in Tris-HCl buffer solution for 6 hours at 24°C, 37°C, and 55°C, respectively.

Sample	Temperature (°C)	Ion concentration (mg/L)				
		Si	Ca	P	Na	Ti
58S	24	3.61 ± 0.03	7.54 ± 0.04	0.06 ± 0.00	—	—
	37	4.97 ± 0.04	10.59 ± 0.02	0.10 ± 0.00	—	—
	55	8.03 ± 0.07	15.80 ± 0.08	0.04 ± 0.00	—	—
58S6N	24	4.45 ± 0.04	3.19 ± 0.09	0.06 ± 0.00	0.86 ± 0.00	—
	37	6.71 ± 0.07	4.81 ± 0.01	0.07 ± 0.00	1.21 ± 0.00	—
	55	10.84 ± 0.09	7.69 ± 0.06	0.03 ± 0.00	1.90 ± 0.00	—
58S6T	24	1.84 ± 0.06	7.33 ± 0.09	0.01 ± 0.00	—	0.001 ± 0.000
	37	2.29 ± 0.08	8.95 ± 0.04	0.07 ± 0.00	—	0.001 ± 0.000
	55	4.93 ± 0.07	13.42 ± 0.10	0.06 ± 0.00	—	0.001 ± 0.000

Table 3: Activation energy of Si ions release from different bioactive glasses in Tris-HCl buffer solution.

Sample	E_a (eV)
58S	0.22
58S6N	0.18
58S6T	0.27

58S6T shows the highest E_a, 0.27 eV, whereas 58S has an intermediate value (0.22 eV) between 58S6N and 58S6T. The dissolution behaviors of the bioactive glasses in Tris-HCl solution for time periods ranging from 1 to 14 days are recorded in Figure 3. It shows that all specimens continue to dissolve after immersion. The resulting weight loss indicated that 58S6N had the highest dissolution rate and solubility compared to other samples over the whole soaking period, reaching up to 21.6% after 14 days. The overall amount of 58S6T dissolution was minimal and reached 12.0% at the end of soaking time. As expected, 58S exhibited an intermediate dissolution behavior between those of 58S6N and 58S6T. In this study, the activation energy of Si ion release and weight loss of the bioactive glass samples were measured to evaluate the *in vitro* degradation of the bioactive glass. Previous studies showed that the lower value of activation energy means a faster release of Si ions [12]. Our results also proved that a faster ionic release was directly related to a low value of activation energy and a faster weight loss. Recent studies have shown that bioactive materials used for either tissue replacement or for tissue regeneration must possess controlled chemical release kinetics that synchronise with the sequence of cellular changes occurring in wound repair [3]. If dissolution rates are too rapid, the ionic concentrations are too high to be effective. If the rates are too slow, the concentrations are too low to stimulate cellular proliferation and differentiation [3]. The results of this study showed that the rate of solubility could be changed or controlled by the substitution of Ca in the 58S bioactive glass with Na or Ti. The differences of dissolution behavior among the three kinds of bioactive glasses also reflected their difference in chemical composition and crystalline structure.

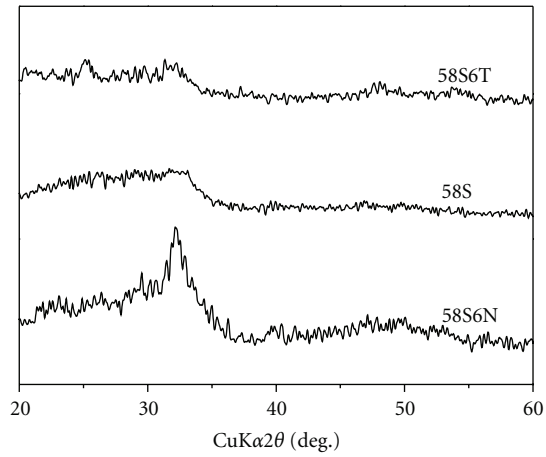

Figure 1: XRD patterns of the samples calcined at 700°C.

3.2. Characterization of Formed Bone-Like Apatite Layer. The capacity of biomaterials to form bone-like apatite could reflect their potential for bonding with bone. The bioactivity is also directly related to the formation of a surface bone-like apatite layer [15]. The XRD patterns of the three specimens after soaking in SBF for 5 days are shown in Figure 4. In order to reduce the interference of the background and noise, XRD patterns have been treated by smoothing. The apatite phase could be detected on all samples. The crystalline peaks of apatite at 31.7° and 25.8° 2θ corresponding to the 211 and 002 reflections of apatite (JCPD 250166) are evident in the XRD patterns. FTIR was used to further elucidate the surface properties of materials. Figure 5 presents the FTIR spectra of the surface layer of the samples soaked in SBF solution for 5 days. As observed, the absorption peaks at 1100, 600, 1400–1550, and 3500 cm^{-1}, corresponding to phosphate (PO_4^{3-}), carbonate (CO_3^{2-}), and hydroxyl

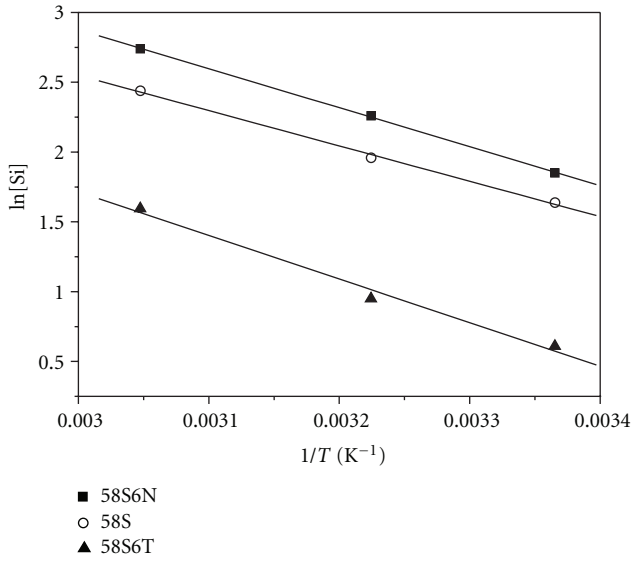

Figure 2: Arrhenius plots for the release of Si ions from different bioactive glasses.

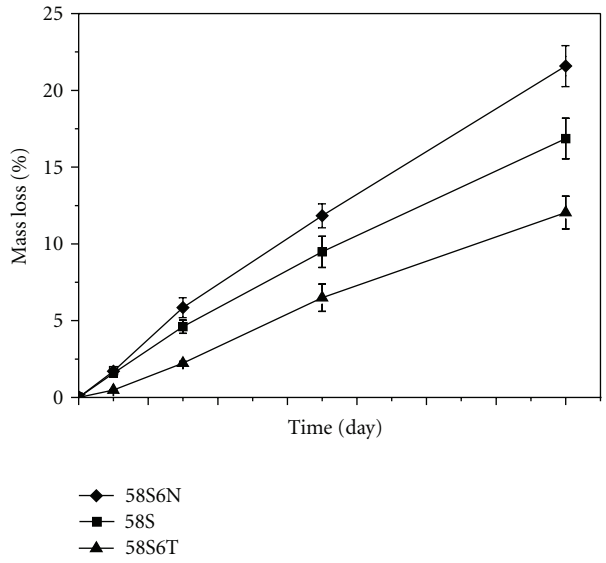

Figure 3: Dissolution behavior of different bioactive glasses in Ringer's solution for 14 days.

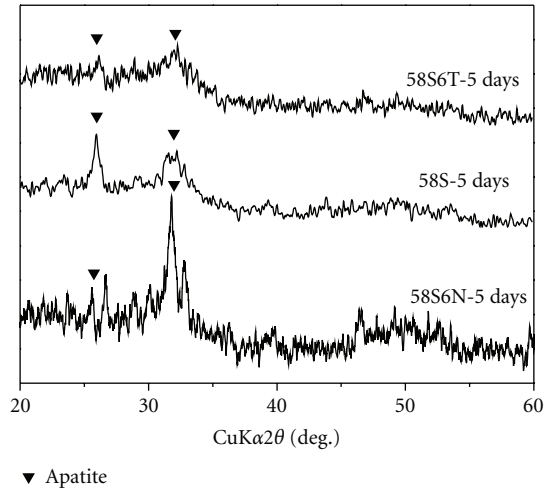

Figure 4: XRD patterns of the 58S, 58S6N, and 58S6T after immersion in SBF for 5 days.

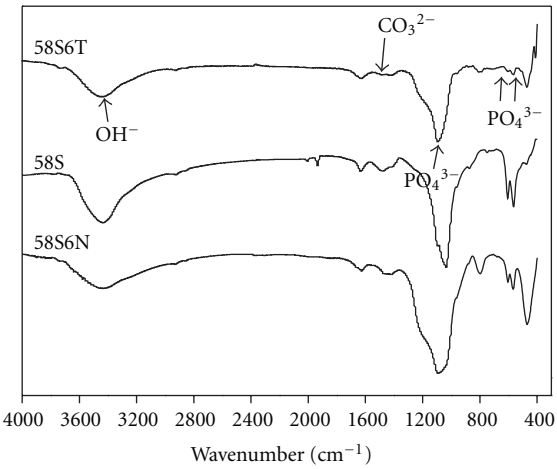

Figure 5: Transmittance FTIR spectra on the surfaces of the 58S, 58S6N, and 58S6T after immersion in SBF for 5 days.

(OH^-), respectively, could be clearly observed from the FTIR spectra after soaking in SBF for 5 days. These results further confirmed that a continuous bone-like apatite layer was formed on the surface of samples after soaking in SBF. To study the effect of Na and Ti on the nucleation of HA on glass samples during the initial soaking periods, the precipitations on glass samples after soaking for 1, 3, and 5 days were observed by an SEM (Figure 6). It can be seen that the precipitated granules with a diameter of about 100 nm distributed homogeneously on the whole surface of 58S glass after immersion for 1 day (Figure 6(a)). The surface of the 58S6N was also observed to be covered by an apatite layer with tiny ball-like shapes after immersion for 1 day (Figure 6(d)). Differently, on 58S6T glass surface, there were only few granules agglomerated with a size of about 1 μm on 58S6T glass (Figure 6(g)). With increasing immersion time (3 and 5 days), the granules on 58S sample grew in size and eventually formed a layer of nanosized crystals with typical morphology of apatite as it occurred on the 58S6N specimens (Figures 6(b), 6(c), 6(e), and 6(f)). However, no obvious change was observed on 58S6T sample surface after immersion for 3 days when compared with that of immersion for 1 day (Figure 6(h)). After 5-day immersion, the surface of 58S6T was observed to be partly covered by an apatite layer with worm-like shapes on the surface (Figure 6(i)). In addition, the changes of pH value in the SBF solution of these three materials were tested, which followed a similar trend during the whole soaking period. The pH value of the SBF solution increased rapidly in the first 6 h and then kept increasing at a relatively lower rate with increasing immersion time up to 7 days. The increment

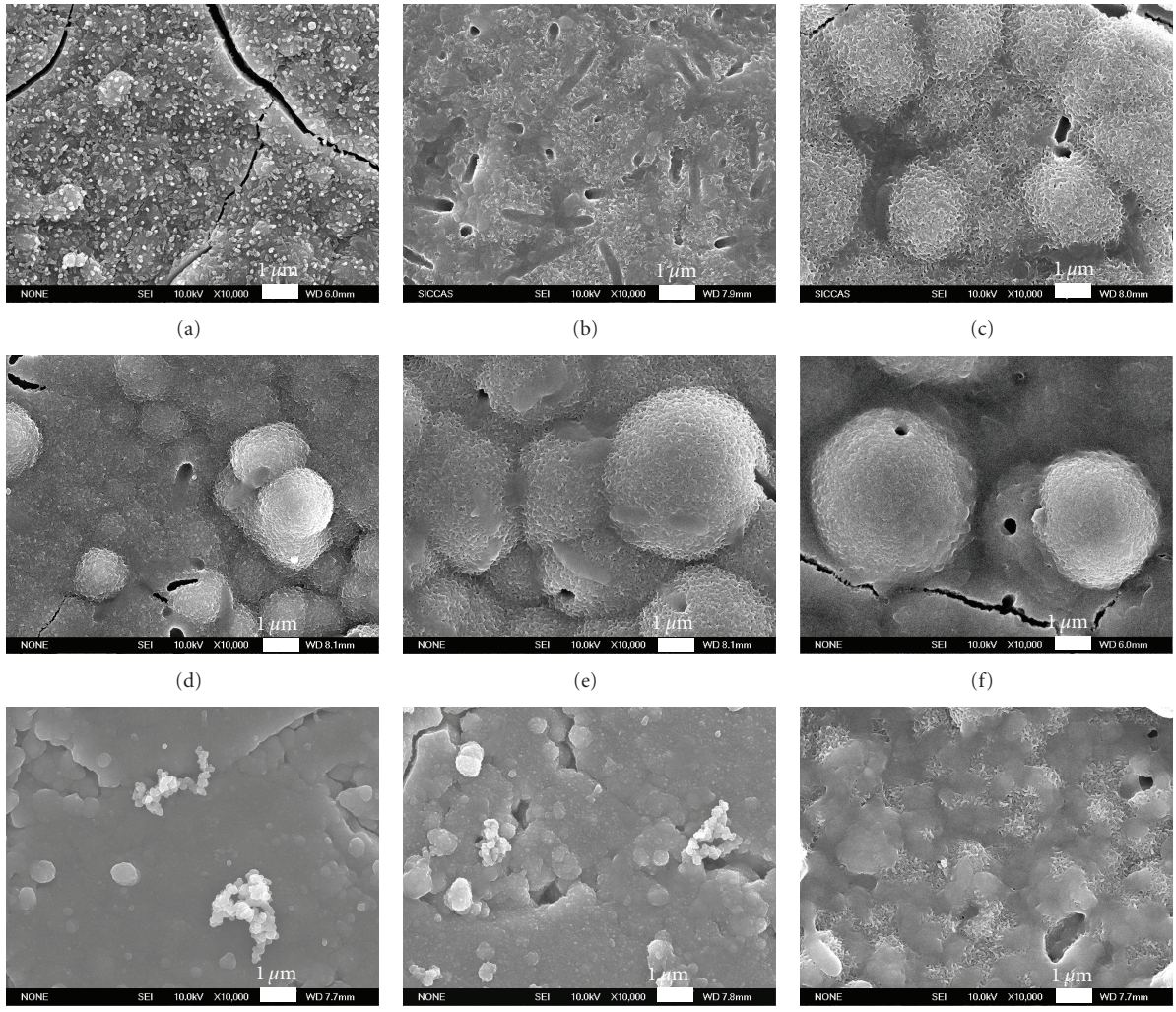

Figure 6: SEM micrographs of the surfaces of 58S ((a), (b), (c)), 58S6N ((d), (e), (f)), and 58S6T ((g), (h), (i)) after immersion in SBF for 1 ((a), (d), (g)), 3 ((b), (e), (h)), and 5 ((c), (f),(i)) days, respectively.

of pH value is maximum for 58S6N (from 7.2 to 9.6 in 7 days), whereas it is minimum for 58S6T (from 7.2 to 7.8 in 7 days). As expected, 58S exhibited an intermediate status (from 7.2 to 8.3 in 7 days). According to the mechanism of apatite formation on the bioactive glass surface, the increment of pH value is mainly caused by Ca and Na release [3]. Previous studies have shown that a higher pH is more favorable for apatite formation [16]. The results in this study are in agreement with this feature. Moreover, it has been reported that the local environment in the initial fracture hematoma is acidic, which later becomes neutral as the healing progresses and, ultimately, alkaline which helps to support differentiation-related events in the healing process [17]. Therefore, pH change at the surrounding glasses may be also helpful to improve their biological performance. Further *in vivo* experiments will be needed to confirm whether this is indeed the case.

In this study, relatively faster dissolution of samples also showed a higher bioactive behavior, which suggested that there would be a relationship between the bioactivity and degradation of these kinds of glasses. It was previously reported that the network connectivity of a glass could be used to predict its solubility and bioactivity. Glass solubility increases as network connectivity is reduced. Glasses of low network connectivity are thus potentially bioactive [8]. In the present study, it can be seen that for every mole of CaO removed from the glass network, one mole of Na_2O must be added in order to maintain the charge balance (Figure 7(a)). Previous studies also indicated that the substitution of CaO for Na_2O does have a marked influence of the degree of packing of the atoms and disrupt the integrity of glass network in glasses. Na_2O is a more effective network disrupting species than CaO [8]. At the same time, it was more difficult for Ca inside the glass samples to release from the network to the solution than Na because of the higher bond energy of Ca–O (110 kJ/mol) as compared to that of Na–O (84 kJ/mol). Therefore, as compared to 58S glass, 58S6N exhibited a faster release of Si ions, a lower

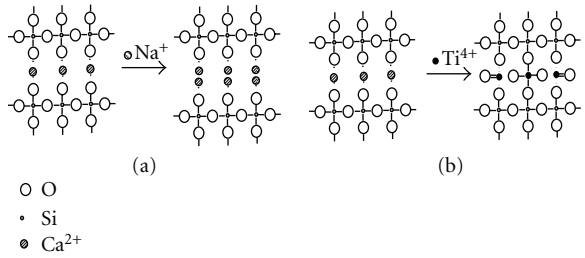

Figure 7: Schematic diagram representing the replacement of Ca ion by Na or Ti ion in 58S sol-gel bioactive glass.

value of activation energy and a faster weight loss. For 58S6T samples, an inverse effect was observed. As Ti is a highly charged tetravalent cation, it presents an intermediate case between tetrahedral cations in a network-forming position and modifier ions [18]. On one hand, Ti can act as a network modifier, disrupting the connectivity of the Si–O–Si network by introducing non-bridging oxygen species (Figure 7(b)) [18]. It has been reported that Ti^{4+} can cross-link the chains more effectively in phosphate glasses owing to its larger charge-to-size ratio and then result in a decrease in solubility [19]. Furthermore, when Ti^{4+} ions substitute for Ca^{2+} ions, O–Ti–O bonds are formed with a strong covalent Ti–O bond than Ca–O bond because the electrostatic field strength of Ti^{4+} is larger than that of Ca^{2+} [9, 20]. On the other hand, due to the same valence as Si, its replacement for Si would assist in the glassy network formation. The introduction of Ti in the 58S glass resulted in the formation of some new interconnections within the basic silicate structural network, as shown in Figure 7(b). Moreover, if Ti^{4+} enters the silicate network, it would create additional bridging oxygens and thereby reduce the glass solubility. Therefore, the structure of 58S6T produced stronger bonds and a closer packing of ions than other two bioactive glasses. In this study, 58S6T could induce apatite formation in SBF, but the rate of apatite formation for them (after 3 days) was slower than that for 58S (with 1 day). These can be related to the more effective cross-linking and higher network connectivity in 58S6T.

4. Conclusions

In this study, the effect of Na and Ti on the *in vitro* degradation behavior and bioactivity in the 58S bioactive glass was evaluated and compared. The Na-containing glass 58S6N accelerated the dissolution rate of the glass, whereas the Ti-containing glass 58S6T slowed down the rate of glass solubility. Na in glass increased the apatite-forming ability in SBF. In contrast, Ti in glass retards the apatite formation at the initial stage of SBF soaking but does not affect the growth of apatite after long periods of soaking. The results of this study indicate that it is possible to engineer the degradation and bioactivity of 58S bioactive glasses by the substitution of Ca in 58S bioactive glass with Na or Ti.

Acknowledgments

This work is supported by the Natural Science Foundation of China (Grant no. 50902020), the Fundamental Research Funds for the Central Universities (Grant no. 2011D10524), and the Opening Foundation of Zhejiang Provincial Top Key Discipline (Grant no. 20110925).

References

[1] R. Li, A. E. Clark, and L. L. Hench, "An investigation of bioactive glass powders by sol-gel processing," *Journal of Applied Biomaterials*, vol. 2, no. 4, pp. 231–239, 1991.

[2] G. S. Polymeris, O. M. Goudouri, E. Kontonasaki, K. M. Paraskevopoulos, N. C. Tsirliganis, and G. Kitis, "Thermoluminescence as a probe in bioactivity studies; the case of 58S sol-gel bioactive glass," *Journal of Physics D*, vol. 44, no. 39, pp. 1–8, 2011.

[3] L. L. Hench, "The story of bioglass," *Journal of Materials Science*, vol. 17, no. 11, pp. 967–978, 2006.

[4] J. Lao, E. Jallot, and J. M. Nedelec, "Strontium-delivering glasses with enhanced bioactivity: a new biomaterial for antiosteoporotic applications?" *Chemistry of Materials*, vol. 20, no. 15, pp. 4969–4973, 2008.

[5] M. Vallet-Regí, A. J. Salinas, J. Román, and M. Gil, "Effect of magnesium content on the *in vitro* bioactivity of CaO-MgO-SiO_2-P_2O_5 sol-gel glasses," *Journal of Materials Chemistry*, vol. 9, no. 2, pp. 515–518, 1999.

[6] A. Balamurugan, G. Balossier, S. Kannan, J. Michel, A. H. S. Rebelo, and J. M. F. Ferreira, "Development and *in vitro* characterization of sol-gel derived CaO-P_2O_5-SiO_2-ZnO bioglass," *Acta Biomaterialia*, vol. 3, no. 2, pp. 255–262, 2007.

[7] M. Laczka, K. Cholewa-Kowalska, A. Laczka-Osyczka, M. Tworzydlo, and B. Turyna, "Gel-derived materials of a CaO-P_2O_5-SiO_2 system modified by boron, sodium, magnesium, aluminum, and fluorine compounds," *Journal of Biomedical Materials Research*, vol. 52, no. 4, pp. 601–612, 2000.

[8] K. E. Wallace and R. G. Hill, "Influence of sodium oxide content on bioactive glass properties," *Journal of Materials Science*, vol. 10, no. 12, pp. 697–701, 1999.

[9] A. S. Monem, H. A. ElBatal, E. M. A. Khalil, M. A. Azooz, and Y. M. Hamdy, "*In vivo* behavior of bioactive phosphate glass-ceramics from the system P_2O_5-Na_2O-CaO containing TiO_2," *Journal of Materials Science*, vol. 19, no. 3, pp. 1097–1108, 2008.

[10] J. P. Zhong and D. C. Greenspan, "Processing and properties of sol-gel bioactive glasses," *Journal of Biomedical Materials Research B*, vol. 53, no. 6, pp. 694–701, 2000.

[11] P. Ducheyne, S. R. Radin, and L. King, "The effect of calcium phosphate ceramic composition and structure on *in vitro* behavior. I. Dissolution," *Journal of Biomedical Materials Research*, vol. 27, no. 1, pp. 25–34, 1993.

[12] D. Arcos, D. C. Greenspan, and M. Vallet-Regí, "A new quantitative method to evaluate the *in vitro* bioactivity of melt and sol-gel-derived silicate glasses," *Journal of Biomedical Materials Research A*, vol. 65, no. 3, pp. 344–351, 2003.

[13] T. Kokubo, H. Kushitani, S. Sakka, T. Kitsugi, and T. Yamamuro, "Solutions able to reproduce *in vivo* surface-structure changes in bioactive glass-ceramic A-W3," *Journal of Biomedical Materials Research*, vol. 24, no. 6, pp. 721–734, 1990.

[14] D. C. Greenspan, J. P. Zhong, and G. P. LaTorre, "Effect of surface area to volume ratio *in vitro* surface reactions of

bioactive glass particulates," *Bioceramics*, vol. 7, pp. 55–60, 1994.

[15] T. Kokubo and H. Takadama, "How useful is SBF in predicting in vivo bone bioactivity?" *Biomaterials*, vol. 27, no. 15, pp. 2907–2915, 2006.

[16] X. Xu and Y. Leng, "Theoretical analysis of calcium phosphate precipitation in simulated body fluid," *Biomaterials*, vol. 26, no. 10, pp. 1097–1108, 2005.

[17] J. Hollinger and M. Wong, "The integrated processes of hard tissue regeneration with special emphasis on fracture healing," *Oral Surgery, Oral Medicine, Oral Pathology, Oral Radiology, and Endodontics*, vol. 82, no. 6, pp. 594–606, 1996.

[18] A. W. Wren, F. R. Laffir, A. Kidari, and M. R. Towler, "The structural role of titanium in Ca-Sr-Zn-Si/Ti glasses for medical applications," *Journal of Non-Crystalline Solids*, vol. 357, no. 3, pp. 1021–1026, 2011.

[19] M. Navarro, M. Ginebra, J. Clément, S. Martínez, G. Avila, and J. A. Planell, "Physicochemical degradation of titania-stabilized soluble phosphate glasses for medical applications," *Journal of the American Ceramic Society*, vol. 86, no. 8, pp. 1345–1352, 2003.

[20] H. Grussaute, L. Montagne, G. Palavit, and J. L. Bernard, "Phosphate speciation in Na_2O-CaO-P_2O_5-SiO_2 and Na_2O-TiO_2-P_2O_5-SiO_2 glasses," *Journal of Non-Crystalline Solids*, vol. 263, no. 1–4, pp. 312–317, 2000.